Journal of proteome research

Article

pubs.acs.org/jpr

PIM2 Kinase Is Induced by Cisplatin in Ovarian Cancer Cells and Limits Drug Efficacy

Daniele Musiani,[†,‡,⊥] Dean E. Hammond,[§,∥] Luca Cirillo,[†,‡] Jessica Erriquez,[‡] Martina Olivero,[†,‡] Michael J. Clague,[§] and Maria Flavia Di Renzo*[,†,‡]

[†]Department of Oncology, University of Torino School of Medicine, 10060 Candiolo (Torino), Italy

[‡]Laboratory of Cancer Genetics, Candiolo Cancer Institute FPO-IRCCS, 10060 Candiolo (Torino), Italy

[§]Cellular and Molecular Physiology, Institute of Translational Medicine, University of Liverpool, L69 3BX Liverpool, United Kingdom

Supporting Information

ABSTRACT: Platinum-based chemotherapy is widely used to treat various cancers, but many patients ultimately relapse due to drug resistance. We employed phosphoproteomic analysis and functional assays of the response of SK-OV-3 ovarian cancer cells to cisplatin as a strategy to identify kinases as candidate druggable targets to sensitize cells to platinum. A SILAC-based approach combined with TiO_2-based phosphopeptide enrichment allowed the direct identification of ERK1/2, p90RSK, and ERBB2 as kinases whose phosphorylation is regulated by cisplatin. Bioinformatic analysis revealed enrichment in linear phosphorylation motifs predicted to be targets of p38MAPK, CDK2, and PIM2. All three PIM kinases were found expressed in a panel of 10 ovarian cancer cell lines, with the oncogenic PIM2 being the most commonly induced by cisplatin. Targeting PIM2 kinase by either biochemical inhibitors or RNA interference impaired cell growth, decreased cisplatin-triggered BAD phosphorylation, and sensitized ovarian cancer cells to drug-induced apoptosis. Overexpression of PIM2 triggered anchorage-independent growth and resulted in increased BAD phosphorylation and cell resistance to DNA damaging agents. The data show that the PIM2 kinase plays a role in the response of ovarian cancer cells to platinum drugs and suggest that PIM inhibitors may find clinical application as an adjunct to platinum-based therapies.

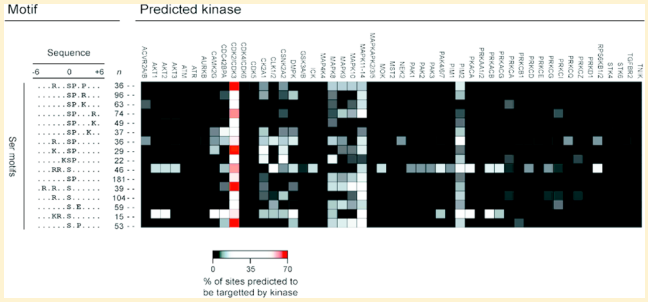

KEYWORDS: *SILAC phosphoproteomics, PIM2 kinase, platinum drugs, ovarian cancer*

INTRODUCTION

The clinical use of platinum compounds was a milestone in the development of successful cancer chemotherapeutic agents.[1] Platinating compounds, including cisplatin, carboplatin, and oxaliplatin, still constitute part of the front-line treatment regimen for patients with many types of cancers, including ovarian, lung, head and neck, testicular, and cervical cancers. They exert anticancer activity through signaling pathways that operate in the cytoplasm and in the nucleus. The best characterized is the formation of platinum−DNA adducts, which primarily cause intrastrand cross-links that activate the DNA damage response and the apoptotic pathway, resulting in cell death.[2] Patients usually have a good initial response to cisplatin-based chemotherapy but later relapse because of the development of platinum resistance, either intrinsic or acquired. This markedly lessens the clinical value of platinum compounds. Several mechanisms account for the platinum-resistant phenotype and include reduced uptake or increased efflux of the platinum drugs due to alterations of transporters, increased glutathione which sequesters the drugs, increased ability to repair DNA damage, or modulation of apoptosis signaling pathways.[3]

Initially, cisplatin-induced DNA lesions trigger the recruitment and activation of the ataxia telangiectasia mutated (ATM) and of the ataxia and RAD related (ATR) kinases, which in turn phosphorylate several key proteins that activate the DNA damage response, leading to cell cycle arrest, DNA repair, or apoptosis.[4] Moreover, cisplatin treatment of cells results in the activation of various branches of the mitogen-activated protein kinase system, including those mediated by extracellular signal-regulated kinases, c-JUN N-terminal kinases, and stress-activated protein kinases.[5,6]

We aimed at gaining global insight into the kinases involved in the response of cancer cells to platinum drugs, as kinases are amenable and druggable targets for therapy. We used quantitative phosphoproteomics, which allows the identification

Special Issue: Proteomics of Human Diseases: Pathogenesis, Diagnosis, Prognosis, and Treatment

Received: June 27, 2014
Published: August 6, 2014

dx.doi.org/10.1021/pr500651n | J. Proteome Res. 2014, 13, 4970−4982

of both kinase substrates and the activated forms of the kinases themselves. The kinase substrates were also subjected to bioinformatic analysis for the prediction of other activated kinases targeting the identified substrates themselves. The study of cells treated with cisplatin allowed the identification of PIM2 as a kinase that is induced by the drug and might interfere with the effectiveness of platinum-based therapies.

EXPERIMENTAL PROCEDURES

Cell Lines and Reagents

The SK-OV-3, NIH-OVCAR-3, OAW42, and OV-90 cell lines derive from serous ovarian carcinomas. IGROV-1, OVCAR-4, and OVCAR-8 cell lines derive from ovarian carcinomas of unknown histotype. The OVCAR-5 cell line derives from an undifferentiated ovarian carcinoma. RMG-1 and TOV-21 G cell lines derive from clear cell ovarian carcinomas. HCT-116 and HT-29 cell lines derive from colorectal carcinomas. The HT-29, OVCAR-4, OVCAR-5, and OVCAR-8 cell lines were from the NCI-60 collection and obtained from Charles River in 2011. RMG-1 cell line was purchased from the Japan Health Science Foundation in 2012. SK-OV-3, OV-90, TOV-21G, NIH-OVCAR-3, IGROV-1, and HCT-116 cell lines were purchased from the American Type Culture Collection (ATCC, Manassas, VA, USA) in 2011. The OAW42 cell line was purchased from the European Collection of Cell Cultures (Sigma-Aldrich, Saint Louis, MO) in 2012. All cell lines were grown according to the manufacturer's instructions. Stable overexpression of PIM2 kinase was carried out using the specific cDNA in lentiviral vector pCCLsin.cPPT.PGK.GFP.WPRE that was kindly provided by Dr. Gagliardi of the Candiolo Cancer Institute. Cisplatin (CDDP) was purchased from Teva Italia (Teva Italia S.r.l., Italy). Trabectedin (ET-743) was purchased from PharmaMar S.A. (Madrid, Spain). Recombinant human hepatocyte growth factor (rhHGF) was purchased from Raybiotech Inc. (Norcross, GA). The CDK1/2 inhibitor SU 9516 and the pan-PIM kinase inhibitors SGI-1776 and CX-6258 were purchased from Calbiochem (EMD Millipore Corporation, Billerica, MA). Doxycycline was purchased from Sigma-Aldrich (Saint Louis, MO).

SILAC Labeling

SILAC labeling and sample preparation were carried out as described.[7] Briefly, SK-OV-3 cells were maintained in RPMI and 10% dialyzed FBS (Dundee Cell Products). To generate light, medium, and heavy SILAC labeled cells, arginine- and lysine-free RPMI was supplemented with 200 mg/L L-proline as well as L-lysine (Lys0) and L-arginine (Arg0), L-lysine-$^{2}H_4$ (Lys4) and L-arginine-U-$^{13}C_6$ (Arg6), or L-lysine-U-$^{13}C_6$-$^{15}N_2$ (Lys8) and L-arginine-U-$^{13}C_6$-$^{15}N_4$ (Arg10) at final concentrations of 28 mg/L for the arginine and 146 mg/L for the lysine amino acids. Approximately 3×10^7 cells were harvested for each experimental set. All of the experiments were carried out at 5% FBS, and cells, where indicated, were pretreated for 48 h with rhHGF (100 ng/mL) before exposure to CDDP (20 μM) for 6 and 24 h.

Sample Preparation

Cells were rinsed with PBS and lysed in SDS-containing buffer (4% SDS, 0.1 M Tris-HCl, pH 7.5). Equal amounts (8 mg) from each experimental condition were combined for subsequent phosphopeptide enrichment. Equal amounts (50 μg) from each experimental condition were combined for subsequent in-gel protein digestion. For pS/pT/pY-peptide isolation, we used the filter-aided sample preparation (FASP)[8] followed by fractionation using strong cation exchange (SCX) chromatography and TiO_2-based phosphopeptide enrichment,[9] as described elsewhere.[7]

LC–MS/MS and Data Processing

Samples were fractionated by nanoscale C18 high-performance liquid chromatography (HPLC) on a Waters nanoACQUITY UPLC system coupled to an LTQ-OrbitrapXL (Thermo Fisher) fitted with a Proxeon nanoelectrospray source, as described previously.[7] The mass spectrometer acquired full MS survey scans in the Orbitrap (R = 30 000; m/z range 300–2000) and performed MSMS on the top 5 multiple charged ions in the linear quadrupole ion trap (LTQ) after fragmentation using collision-induced dissociation (30 ms at 35% energy). Full scan MS ions previously selected for MS/MS were dynamically excluded for 180 s from within a rolling exclusion list (with n = 1). All spectra were acquired using Xcalibur software (version 2.0.7; Thermo Fisher Scientific).

Raw MS peak list files from each experimental configuration were searched against the human IPI database (version 3.77) using the Andromeda search engine[10] and processed with the MaxQuant software suite (version 1.2.2.5).[11] The minimum required peptide length was set to 6 amino acids, and two missed cleavages were allowed. Cysteine carbamidomethylation was set as a fixed modification, whereas oxidation and S/T/Y phosphorylation were considered as variable modifications. The initial precursor and fragment ion maximum mass deviations in the database search were set to 7 ppm and 0.8 Da, respectively. Peptide and protein false discovery rates were set to 0.01. Proteins with at least one peptide unique to the protein sequence were considered as valid identifications.

Cluster Analysis of Shortlists and Gene Ontology (GO) Terms

GProX was used to analyze the data set produced by MaxQuant.[12] SILAC ratios were $\log_2$-transformed and subjected to unsupervised clustering based on the fuzzy cmeans algorithm.[13] The data was grouped in 6 clusters (fuzzification value set = 2; regulation threshold = ±0.58; 100 iterations of the algorithm performed). Bioinformatic information was then retrieved, through GProX, from the UniProt database, and possible enrichment of biological features in the 6 clusters was assessed (specifically, GO molecular function and GO biochemical processes annotations, plus the frequency of protein domains within the Pfam_UniProt database). For the identification of over-represented GO terms, a binomial statistical test was used with a Benjamini and Hochberg p-value threshold set at 0.05 (minimum number of occurrences of the GO term in the cluster = 2; background = 0; lowest hierarchical rank = 2). For the enrichment of Pfam annotated protein domains, the Fischer's exact test was employed with a Benjamini and Hochberg p-value threshold set to 1.0.

Linear Kinase Motif Analysis

Phosphopeptides with a phosphorylation localization probability >0.75 (class 1 sites) were analyzed for common motifs and their putative regulatory kinases. Sequence windows comprising ±6 amino acids adjacent to the phosphosite were extracted from the data set. A partially degenerate amino acid code was used as described[14] to group Arg and Lys, Glu and Asp, and nonphosphorylated Ser and Thr residues. The list was submitted to Motif-X[15] to identify over-represented motifs versus the IPI human proteome (occurrence limit = 1% of

dx.doi.org/10.1021/pr500651n | J. Proteome Res. 2014, 13, 4970–4982

submitted sequence windows, *p*-value threshold = 1×10^{-6}). In parallel, the full protein sequence and phosphosite for all class 1 phosphopeptides were submitted to NetworKIN v2.046 to identify putative kinase regulators of these sites.[16] We extracted the subset of phospho-proteins that were significantly responsive to CDDP. Proteins were grouped according to their motifs identified by Motif-X, and the percent of the total within each group putatively regulated by each kinase was calculated and plotted as a heatmap. To indicate the overall regulation of sites associated with each motif, average CDDP ratios were normalized by assigning the maximum observed increase in phosphorylation a value of 1 and the maximum decrease a value of −1.

Western Blot Analysis

Western blot analysis was carried out as described.[17] The mouse monoclonal anti-vinculin and rabbit polyclonal anti-P-BAD (Ser155) were from Sigma-Aldrich (Saint Louis, MO). The mouse polyclonal anti-P-Erk1/2 (Thr202/Tyr204), rabbit monoclonal anti-P-ERBB2 (Tyr1221/Tyr1222), anti-PIM1, anti-PIM2, anti-PIM3, anti-P-BAD (Ser112), anti-BAD, anti-Erk1/2, anti-c-Myc, rabbit polyclonal anti-P-p38 MAPK (Thr180/Tyr182), rabbit polyclonal anti-ERBB2, anti-p38 MAPK, anti-cleaved PARP (Asp214), anti-P-Stat3 (Tyr705) and anti-Stat3 were all obtained from Cell Signaling Technology (Beverly, MA). Mouse monoclonal anti-γH2A.X (Ser139) was obtained from Millipore (EMD Millipore Corporation, Billerica, MA). Bound antibodies were detected using the appropriate peroxidase-conjugated secondary antibody and revealed by enhanced chemiluminescence (Pierce, Rockford, IL).

Quantitative PCR and Cloning

Quantitative PCR was carried out as described.[18] Primer sets used were as follows: *PIM1* FW: TTCGGCTCGGTCTACTCAGG, RV: TTAGGCAGCTCTCCCCAGTC; *PIM2* FW: ACTCCAGGTGGCCATCAAAG, RV: TCCATAGCAGTGCGACTTCG; *PIM3* FW: CACTGCCACAGCTGCGG, RV: CGCACCCGAACCGAAGT; cyclophilin A FW: CATCCTAAAGCATACGGGTCC, RV: TTCTTGCTGGTCTTGCCATTC. PCR cycling conditions were as follows: 30 s at 95 °C 30, 5 s at 95 °C followed by 15 s at 60 °C (40 cycles), 30 s at 95 °C, 10 s at 65 °C plus 10 s at 0.5 °C (60 cycles: melting curve). Total cellular RNA was isolated using the SV total RNA isolation kit (Promega, Fitchburg, WI). To quantify the expression levels of each *PIM* gene, equal amounts of cDNA were synthesized using the Moloney murine leukemia reverse transcriptase (Promega, Fitchburg, WI) and mixed with SsoFast EvaGreen Supermix (Bio-Rad, Hercules, CA) and 300 mM of each of the respective forward and reverse primers. Quantitative real-time PCR was done on a MyiQ thermal cycler (Bio-Rad, Hercules, CA). Each target gene's expression was evaluated using a relative quantification approach, with cyclophilin A (GenBank accession NM_021130) as an internal reference. Drugs were used at the indicated doses, and RNA was extracted from each time point for the indicated time.

PIM2 cDNA was amplified starting from cDNA of SK-OV-3 obtained as above. The primers used were as follows: FW: GGGGATCCCCCGGGCTGCAGATGTTGACCAAGCCTCTACAGGGGCCTC and RV: GAGGTTGATTGTCGACTTAGGGTAGCAAGGACCAGGCC. The PIM2 cDNA was cloned into the pCCLsin.cPPT.PGK.GFP.WPRE lentiviral vector, after plasmid linearization with *Pst*I and *Sal*I using the in-fusion HD EcoDry cloning plus according to the manufacturer's instructions (Clontech Laboratories, Inc., CA). The GFP cassette was removed from the vector after digestion with *Xho*I.

RNA Interference

Stable silencing of *PIM2* was achieved using the *PIM2*-specific human TRIPZ lentiviral (LV)-inducible shRNA (clone V2THS_77585; Open Biosystems, Huntsville, AL).

Cell Transduction with Lentiviral Vectors

Cells were transduced using second-generation lentiviral vectors, whose stocks were produced by transient transfection of 293T cells with the packaging plasmid pCMV-deltaR8.74, the envelope plasmid pMD2G-VSVG, and the respective transfer gene carrying vector. Serial dilutions of freshly harvested conditioned medium were used to infect 10^5 cells in a 6-well plate in the presence of polybrene (8 μg/mL). Control cells were generated by transduction with the same empty lentiviral vector.

Apoptosis assay

Caspase activation was determined by labeling cells with anti-active caspase-3 antibody (BD PharMingen, San Diego, CA) followed by a PE-conjugated goat anti-rabbit Ig (BD PharMingen, San Diego, CA). Cells were fixed and permeabilized with BD Cytofix/Cytoperm (Becton Dickinson, Franklin Lakes, NJ) according to the manufacturer's instructions. Apoptosis was also measured by staining cells with allophycocyanin (APC)-conjugated Annexin V (Bender MedSystems, Burlingame, CA) and propidium iodide (Invitrogen, Eugene, OR), which allows detection of phosphatidylserine (PS) exposure on the cell surface and the loss of plasma membrane integrity, respectively. The samples were analyzed on a CyAN-Adp flow cytometer (Dako, CO). Data acquisition was performed using Summit software (Dako, CO).

Soft Agar and Cell Viability Assay

SK-OV-3 (3000 cells/well) and OVCAR-8 (2000 cells/well) cells were seeded in triplicate in 6-well plates on a 0.5% SeaPlaque agar layer (Lonza, Walkersville, MD). The plates were incubated for 4 and 2 weeks for SK-OV-3 and OVCAR-8 cell lines, respectively. Colonies were stained with MTT salts (Sigma-Aldrich, Saint Louis, MO), photographed, and counted using NIH ImageJ (W. Rasband, NIH) software. Three independent experiments were performed.

Viability assay of ovarian cancer cells treated with the indicated drugs for the indicated amounts of time was determined using the CellTiterGlo proliferation kit (Promega, Fitchburg, WI) according to the manufacturer's protocol.

Statistical Analysis

Statistical analysis of the data was performed using ANOVA (Microsoft Excel; Microsoft, Redmond, WA, USA).

The Cancer Genome Atlas Analysis

Using the cBioPortal,[19] mutations and copy number alterations (CNA) of the PIM2 gene in ovarian serous cystadenocarcinoma samples studied by the The Cancer Genome Atlas Network were analyzed (http://www.cbioportal.org/public-portal/index.do?cancer_study_id=ov_tcga&genetic_profile_ids_PROFILE_MUTATION_EXTENDED=ov_tcga_mutations&genetic_profile_ids_PROFILE_COPY_NUMBER_ALTERATION=ov_tcga_gistic&genetic_profile_ids_PROFILE_MRNA_EXPRESSION=ov_tcga_rna_seq_v2_mrna_median_Zscores&Z_SCORE_THRESHOLD=2.

dx.doi.org/10.1021/pr500651n | J. Proteome Res. 2014, 13, 4970−4982

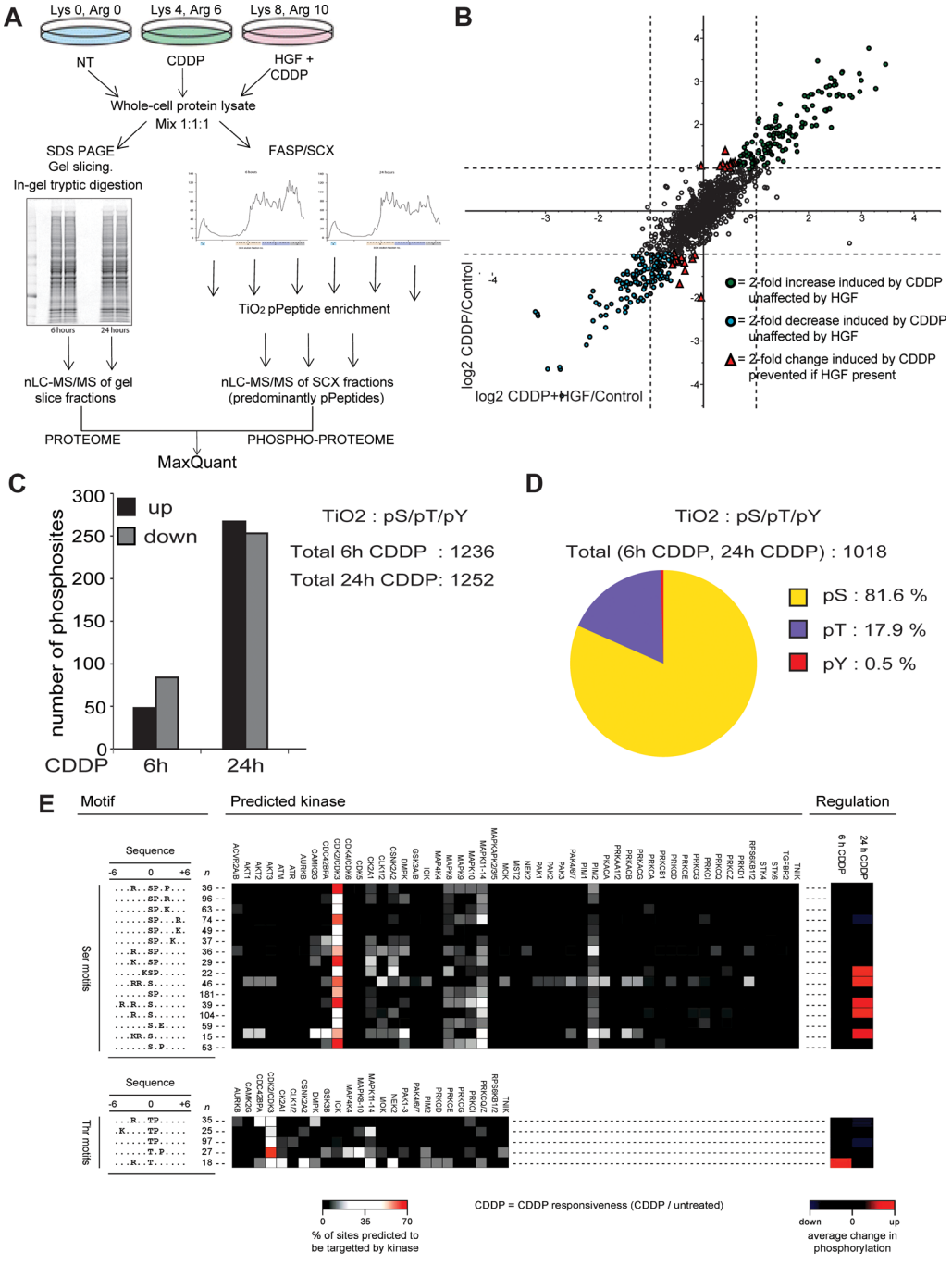

Figure 1. (A) Schematic workflow of the triplexed configuration of the experiments showing the purification modes both for proteomic and phosphoproteomic analysis. (B) Scatter plot showing how the abundance of the phosphosites identified in the TiO_2 was modulated by CDDP and by the combined treatment HGF + CDDP (HGF, 100 ng/mL for 48 h; CDDP, 20 μM for 24 h). (C) Number of phosphosites identified in the TiO_2 samples that were significantly over- and under-represented following treatment with CDDP (20 μM) for 6 and 24 h, respectively. (D) Percentage of pS, pT, and pY carrying peptides identified following phosphopeptides enrichment. (E) List of over-represented linear phosphorylation motifs extracted from the set of phosphopeptides using Motif-X software (left panel). The number (n) of phosphopeptides matching each motif is indicated. Matrix shows the candidate kinases for these motifs, predicted using NetworKIN. The right panel shows the average response associated with each motif in response to CDDP treatment.

0&RPPA_SCORE_THRESHOLD=2.0&data_priority=0&case_set_id=ov_tcga_all&case_ids=&gene_set_choice=user-defined-list&gene_list=PIM2&clinical_param_selection=null&tab_index=tab_visualize&Action=Submit) and compared to alterations found in all cancer types (http://www.cbioportal.org/public-portal/cross_cancer.do?cancer_study_id=all&genetic_profile_ids_PROFILE_MUTATION_EXTENDED=ov_tcga_mutations&genetic_profile_ids_PROFILE_COPY_NUMBER_ALTERATION=ov_tcga_gistic&genetic_profile_ids_PROFILE_MRNA_EXPRESSION=ov_tcga_rna_seq_v2_mrna_median_Zscores&Z_SCORE_THRESHOLD=2.0&RPPA_SCORE_THRESHOLD=2.0&data_priority=0&case_ids=&gene_set_choice=user-defined-list&gene_list=PIM2&clinical_param_selection=null&tab_index=tab_visualize&Action=Submit#crosscancer/overview/0/PIM2).

dx.doi.org/10.1021/pr500651n | J. Proteome Res. 2014, 13, 4970−4982

Table 1. Lists of the Top 50 Up- (Left) and Downregulated (Right) Phosphosites Following 24 h CDDP Treatment (20 μM) of SK-OV-3 Cells

gene symbol	phosphorylation position	SILAC ratio M/L	gene symbol	phosphorylation position	SILAC ratio M/L
H2A.X	140	12.619	HNRPLL	68	0.032321
TMPO	433	11.512	ERBB2	1054	0.052858
S100A13	32	10.303	SRGAP1	932	0.077862
NOP56	563	9.4318	LASP1	104	0.082726
RPS20 40S	9	9.3445	SEPT9	49	0.084763
TRIM28	473	9.1525	SMAD2	8	0.11839
HIST1H1C	36	8.492	SQSTM1	269	0.13252
HMGA1	39	8.0107	BAT2	782	0.14
HMGN1	7	8.0019	AGFG1	177	0.18297
GTF2I	784	7.8764	TMPO	306	0.18436
SH3GL1	298	7.7634	LMNA	19	0.19248
RANBP2	1509	7.5123	LMNA	22	0.19248
RTN4	107	7.4245	BAT2L2	2675	0.19379
HIST1H1E	37	7.131	ADD1	617	0.19828
PTRF	167	6.741	H2AFY	129	0.20294
PSMA5	56	6.729	MAP7D1	399	0.20692
SRRM1	781	6.6446	ELAVL1	229	0.21122
VIM	73	6.6358	MAP1B	2271	0.21161
HMGA1	44	6.4513	CLTC	394	0.21606
SNX1	188	6.3006	PPP1R13L	280	0.22523
PPIG	696	6.2914	MAP4	2218	0.23035
CLTA	105	6.2781	AHNAK	637	0.23084
PTRF	169	6.257	OCIAD1	113	0.23325
HCFC1	666	6.2518	SRGAP1	906	0.23534
MAP1B	561	6.1645	LARP4B	732	0.23974
PPP1R12A	299	6.1381	LARP4B	736	0.23974
PNN	66	6.114	PARP4	1335	0.24138
AHNAK2	1112	6.1124	ZDHHC5	398	0.24958
BAD	118	5.6775	HNRNPA1	2	0.25334
GIGYF2	223	5.2316	AHNAK	5739	0.25642
PPP1R12A	507	5.2301	NCL	121	0.26202
VPS26B	304	5.1493	RALY	119	0.26455
EPB41L2	598	5.0998	PPP1R1B	75	0.26459
PHF3	567	5.0823	PSIP1	141	0.27333
PHF3	574	5.0823	SPTAN1	1031	0.27485
SF3B2	343	4.8012	ERBB2	1078	0.28102
STMN1	38	4.7945	ERBB2	1083	0.28102
AHNAK	3426	4.5956	SEC61B	7	0.29316
LMNB1	20	4.5651	PDLIM5	111	0.29364
PTRF	300	4.5576	MAP4	375	0.29573
UGDH	476	4.4537	SEC61B	17	0.29589
NUCKS1	54	4.3301	NUCKS1	179	0.30374
AHNAK2	5175	4.2008	MAP2	1649	0.30471
AHNAK	2397	4.0703	SPAG9	203	0.30632
RAI14	252	4.0435	SPTAN1	1029	0.30667
CLIP1	348	4.0253	AHNAK	5749	0.31337
MAPK1	185	3.9175	HIST1H1D	18	0.31365
TNKS1BP1	1385	3.858	SEPT9	82	0.31463
DENND5B	868	3.8571	ERBB2	1103	0.3183
AHNAK	1452	3.8524	DDX21	89	0.31865

RESULTS

SILAC-Based Phosphoproteomic Analysis of Ovarian Cancer Cells Treated with CDDP

We used SILAC (stable isotope labeling by amino acids in cell culture) in combination with high-resolution mass spectrometry[20] to study the dynamic response of the phosphopeptide network to cisplatin in ovarian cancer cells. We studied the proteomic and phosphoproteomic profiles of the p53-defective SK-OV-3 ovarian cancer cells, which are described as being partially resistant to cisplatin (CDDP) treatment with an IC_{50} of about 13 μM.[21,22] We previously showed that long-term (72 h) treatment with 10 μM CDDP induced the apoptotic death of approximately 30% of cells and that long-term pretreatment with hepatocyte growth factor (HGF) increased cell susceptibility to CDDP-induced apoptosis.[23] Thus, we treated SK-OV-3 cells, labeled to equilibrium with distinct isotopic forms of

dx.doi.org/10.1021/pr500651n | J. Proteome Res. 2014, 13, 4970−4982

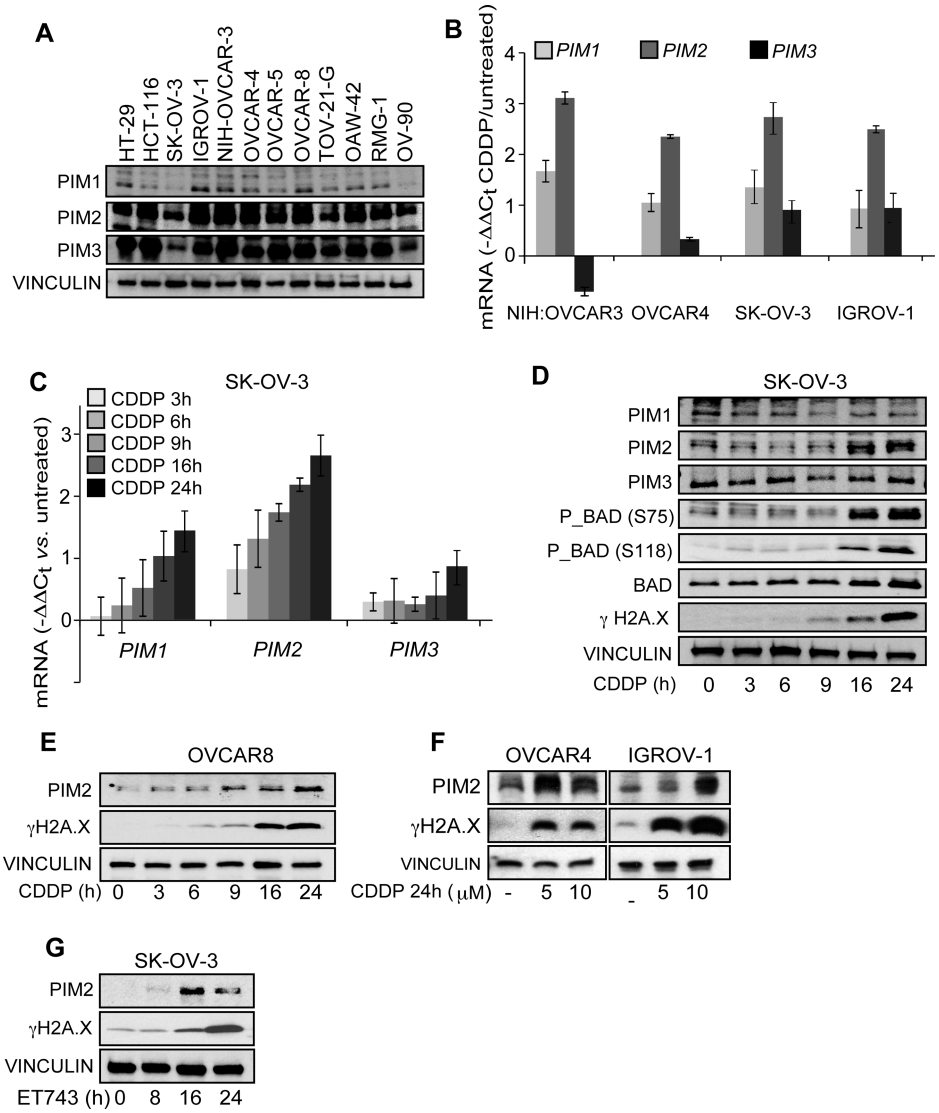

Figure 2. (A) Western blot analysis showing that the PIM kinases are expressed in a panel of 10 ovarian cancer cell lines. HT-29 and HCT-116 colorectal cancer cells were used as positive controls. Notably, alternative initiation sites have been reported for PIM1 and PIM2, which allow for the generation of different proteins of 34 and 40 kDa and 34, 37, and 40 kDa, respectively. The two longest PIM2 isoforms (37 and 40 kDa) are visible in this and in the subsequent blots. (B) Quantitative real-time PCR (qPCR) showing the expression of *PIM1*, *PIM2*, and *PIM3* genes in response to 24 h CDDP treatment in a panel of ovarian cancer cell lines. Different concentrations of CDDP were used according to the different drug susceptibility of each cell line: 20 μM for NIH-OVCAR3 and SK-OV-3, 10 μM for IGROV-1, and 5 μM for OVCAR4. (C) Time-course analysis by qPCR showing that only PIM2 expression was significantly induced following shorter CDDP (20 μM) treatment of SK-OV-3 cells. (D–F) Western blot analysis showing that CDDP treatment induced PIM2 protein expression (D–F) and BAD phosphorylation at S75 and S118 (D) in ovarian cancer cells. SK-OV-3 (D), OVCAR-8 (E), and OVCAR-4 and IGROV-1 (F) cells were exposed to the indicated concentrations of CDDP (μM) for the indicated time (h). (G) SK-OV-3 cells were exposed to trabectedin (ET743 0.5 nM) for the indicated time (h). The phosphorylated form of histone H2A.X (γH2A.X) is shown as a measure of DNA damage. The blots were reprobed with vinculin antibody to confirm equal loading.

arginine and lysine, with CDDP for 6 and 24 h, with and without HGF pretreatment (Figure 1A). Then, we carried out the proteome and phosphoproteome analyses according to the workflow indicated in Figure 1A. Phosphopeptides were purified and then analyzed using liquid chromatography coupled with tandem mass spectrometry (LC–MS/MS).[9] In parallel, in-gel digestion of proteins resolved by SDS-PAGE was performed to investigate the CDDP and CDDP + HGF response of the whole proteome.

The scatter plot in Figure 1B shows that CDDP dictated a clear phosphoproteomic signature in SK-OV-3 ovarian cancer cells that was only minimally fine-tuned by HGF coapplication. In fact, only very few phosphopeptide changes were associated with the addition of HGF to CDDP. Thus, we focused our attention on the response of ovarian cancer cells to the drug alone.

In our phosphopeptide data set, we identified over 1000 phosphorylation sites belonging to 445 proteins in both SK-OV-3 cells treated with CDDP for 6 h and in those treated for 24 h (Supporting Information Table S1). Figure 1C shows the number of the detected phosphosites that were considered either CDDP upregulated or CDDP inhibited, as defined by >1.5 or <0.67 fold change in enrichment, respectively, following stimulation with the drug for 6 and 24 h. Changes in cellular phosphorylation status were evident at 6 h but showed enhancement with a longer time of treatment.

dx.doi.org/10.1021/pr500651n | J. Proteome Res. 2014, 13, 4970–4982

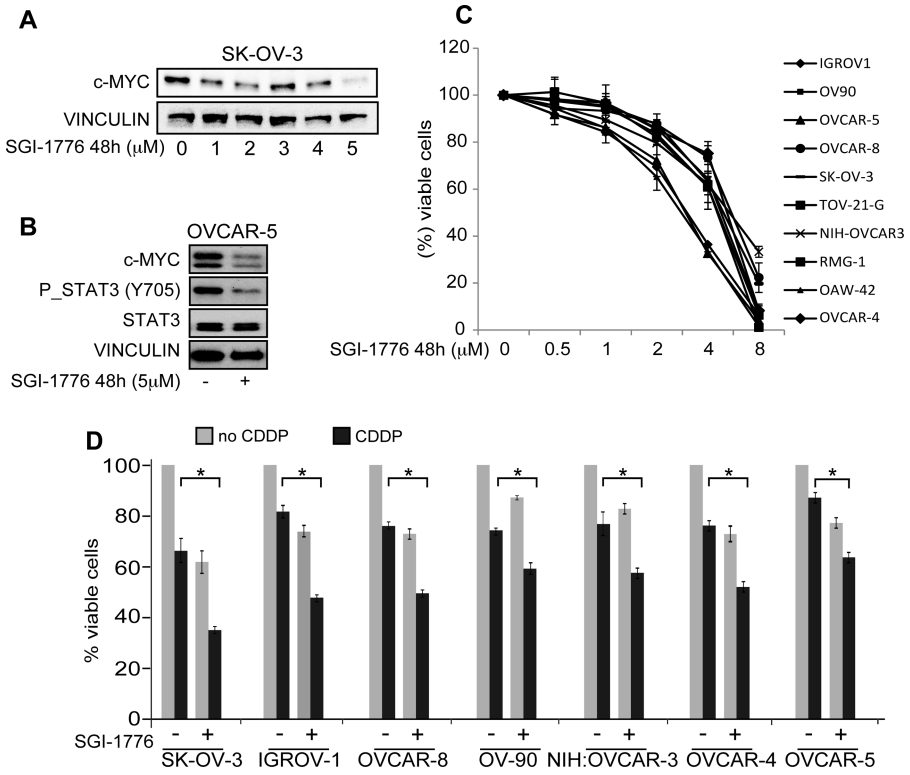

Figure 3. (A, B) Western blot analysis showing Myc protein expression (A, B) and STAT-3 phosphorylation (B) after the treatment of SK-OV-3 (A) and OVCAR-5 (B) ovarian cancer cell lines with the specific pan-PIM inhibitor SGI-1776 for 48 h at the indicated doses. (C) Viability of the listed ovarian cancer cell lines after the treatment with SGI-1776 for 48 h. (D) Viability of the listed cell lines after the treatment with SGI-1776 and CDDP. Cells were treated for 48 h with different concentrations of SGI-1776 and CDDP according to the drug susceptibility of each cell line, i.e., SGI-1776 was 4 μM for SK-OV-3, OVCAR-8, and OVCAR-4 and 2 μM for IGROV-1, OV-90, NIH-OVCAR-3, and OVCAR-5; CDDP was 2 μM for IGROV-1; 3 μM for NIH-OVCAR-3 and OVCAR-4; 4 μM for SK-OV-3, OV-90, and OVCAR-5; and 8 μM for OVCAR-8.

Figure 1D shows the percentage of phospho-serine/phospho-threonine/phospho-tyrosine (pS/pT/pY) carrying peptides identified in the data set corresponding to both time points.

The analysis of all peptides (7216) from the in-gel separation reveals a substantive change in levels for only 10 out of 718 proteins following 24 h CDDP treatment (Supporting Information Table S2). This suggests that changes in phosphopeptides are primarily due to specific activity of phosphorylation rather than protein abundance.

Among the phosphosites upregulated by CDDP (Table 1), direct targets of ATM/ATR were identified. Because it is known that CDDP-induced DNA damage activates these kinases, their targets were considered as a positive control. Indeed, the most upregulated phosphosite in the 24 h treatment data set was serine 139 of the histone H2A.X. Another identified ATM substrate was serine 473 of the transcriptional repressor TRIM28/KAP1.[24]

Among the phosphosites regulated following 24 h CDDP treatment, some (4%) of them belonged to the following kinases: ERBB2, MAPK1, p90RSK, CDK12, MARK2, ABL2, MRCK, MAST2, MAP3K2, PRKAA1, CKB, PFKBF2, MARK3, MARCKS, PFKL, PI4KB, and MAP2K2. However, for all of the above kinases except MAPK1, the respective identified phosphosites did not lie within the activation loop of the kinase domain, i.e., they cannot be used as a proxy for their kinase activity.[25] Therefore, we also looked for linear phosphorylation motifs that are over-represented within our phosphopeptide data set using the Motif-X tool[15] (Figure 1E, left panel). This catalog was then used to generate a list of candidate kinases that could phosphorylate these motifs using the NetworKIN algorithm that weights its prediction according to known protein−protein interactions contained in the STRING database. As shown in Figure 1E (central panel), CDK2/CDK3, MAPK 8−10 (also known as JNKs), MAPK 11−14 (also known as p38MAPK isoforms), and the PIM2 kinase were predicted to be the candidate kinases for most of the pS and pT motifs enriched in our data set. Among the identified phosphosite-carrying motifs, some were found to be upregulated following CDDP treatments (Figure 1E, right panel).

We performed a hierarchical clustering analysis of the responsive set of proteins/peptides and found 6 groups corresponding to distinct patterns of response to the time course of drug treatment (Supporting Information Figure S1A). The proteins of each cluster were sequentially compared to the much larger set of unresponsive proteins for the enrichment of gene ontology (GO) terms relating to molecular functions (MF) and biochemical processes (BP) as well as for protein domains within the Pfam_UniProt database, and the results were displayed as heat maps (Supporting Information Figure S1B−D). The heat map of the GO BP terms indicated that cluster 1 is enriched for proteins involved in the progression of the cell cycle and in the negative regulation of DNA double-strand break repair. The analysis also suggested that molecules involved in the Toll-like receptor signaling pathway were enriched among proteins displaying reduced phosphorylation upon CDDP treatment and thus belonged to cluster 3.

dx.doi.org/10.1021/pr500651n | J. Proteome Res. 2014, 13, 4970−4982

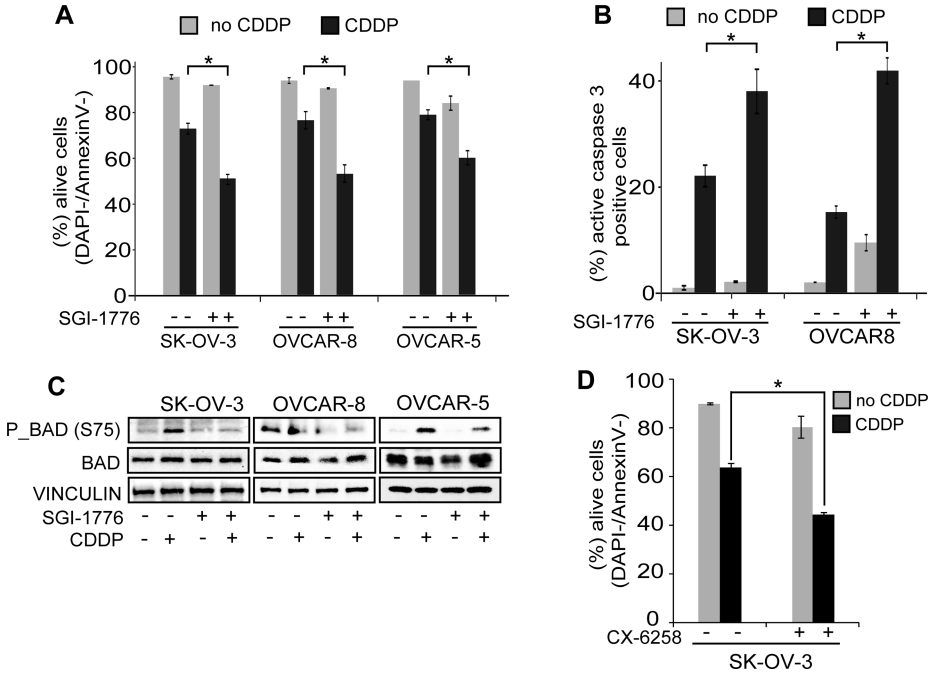

Figure 4. (A, B) Apoptotic death of the indicated ovarian cancer cell lines following exposure to CDDP for 48 h according to the drug susceptibility of each cell line (see Experimental Procedures), evaluated as percentage of living cells labeled with neither DAPI nor AnnexinV (A) or dead cells labeled with an active caspase-3 antibody (B); labeled cells were measured using flow cytometry. Where indicated, cells were pretreated for 3 h with SGI-1776 (3 μM). (C) Western blot analysis showing BAD phosphorylation after CDDP treatment with or without cell pretreatment with SGI-1776 (3 μM). Cells were exposed to CDDP for 24 h according to the drug susceptibility of each cell line, as above. (D) Apoptotic death of SK-OV-3 cells treated with CDDP (20 μM) with or without the pan-PIM inhibitor CX-6258 (2 μM) for 48 h. The blots were reprobed with vinculin antibody to confirm equal loading. Cell viability was measured using CellTiter Glo assay. Mean ± standard deviation, n = 3. Statistical significance was determined using ANOVA test: *P < 0.05.

Altogether, the phosphoproteome analyses showed that a number of potentially important kinases are regulated in cells committed to death by CDDP.

Functional Validation of the Candidate Kinases Regulated by CDDP in Ovarian Cancer Cell Lines

Our phosphoproteomic analysis suggested that a number of kinases might play a role in the response of cancer cells to CDDP. The possible role of ERBB2, ERK1/2, p38MAPK, JNKs, and CDK2 in cell response to platinum has been already shown.[17,26−28] We validated biochemically and functionally our phosphoproteomic data on these kinases in ovarian cancer cells (Supporting Information Figure S2).

The possible role of the PIM2 kinase in ovarian cancer cells and in the cell response to CDDP was a novelty. The family of PIMs[29,30] consists of three highly homologous kinases (PIM1, PIM2, and PIM3). Figure 2A shows that all three kinases are expressed in a panel of 10 ovarian cancer cell lines, representative of different histotypes. The treatment of ovarian cancer cell lines with CDDP resulted in the increased expression of at least one of the PIM kinases, with PIM2 being the most consistently increased at both the mRNA (Figure 2B) and protein levels (Figure 2D−F), even after a short treatment with CDDP (Figure 2C). We found that the upregulation of PIM2 expression by CDDP was associated with the increased phosphorylation of its substrate BAD on serine 75 (corresponding to the serine 112 of mouse bad) and serine 118 (corresponding to the serine 155 of mouse bad) (Figure 2D). BAD phosphosites serine 118 and serine 99 were also identified in our phosphopeptide data set as upregulated in CDDP treated cells, as noticeable in Table 1 and Supporting Information Table S1, respectively. Interestingly, another DNA damaging agent, trabectedin, induced a similar increase in PIM2 expression (Figure 2G).

Thus, we focused our attention onto the possible functional role of PIM2 in ovarian cancer cells and first used a pan-PIM specific biochemical inhibitor (SGI-1776[31]). Figure 3A,B shows that PIM inhibition resulted in reduced protein levels of c-MYC and reduced phosphorylation of STAT3, which are among the best characterized targets of the PIM1 and PIM2 kinases.[32−34] SGI-1776 impaired the viability of ovarian cancer cells (Figure 3C) and synergized with CDDP not only in reducing cell viability (Figure 3D) but also in inducing apoptosis, as measured by Annexin V binding and DAPI staining (Figure 4A) and active caspase-3 staining (Figure 4B). In agreement, pretreatment of ovarian cancer cells with SGI-1776 impaired CDDP-triggered BAD phosphorylation (Figure 4C). A similar effect was elicited by a structurally unrelated pan-PIM inhibitor, CX-6258 (Figure 4D).

Silencing of *PIM2* (Figure 5A,D) impaired the growth as monolayer cultures and in semisolid medium of both SK-OV-3 (Figure 5B−C) and OVCAR-8 (Figure 5E−F) cells. Silencing of *PIM2* also showed that it was required to protect cells from death induced by CDDP, as shown by reduced viability (Figure 6A) and increased Annexin V and DAPI staining (Figure 6B) and PARP cleavage (Figure 6C) in PIM2-silenced cells in comparison to that in control cells. In agreement, PIM2 silencing also impaired BAD phosphorylation triggered by CDDP (Figure 6D).

Overexpression of PIM2 (Figure 7A) was able to protect cells from apoptosis triggered by CDDP and trabectedin (Figure 7B) and, accordingly, triggered BAD phosphorylation (Figure 7A). Overexpression of PIM2 resulted per se in an

dx.doi.org/10.1021/pr500651n | J. Proteome Res. 2014, 13, 4970−4982

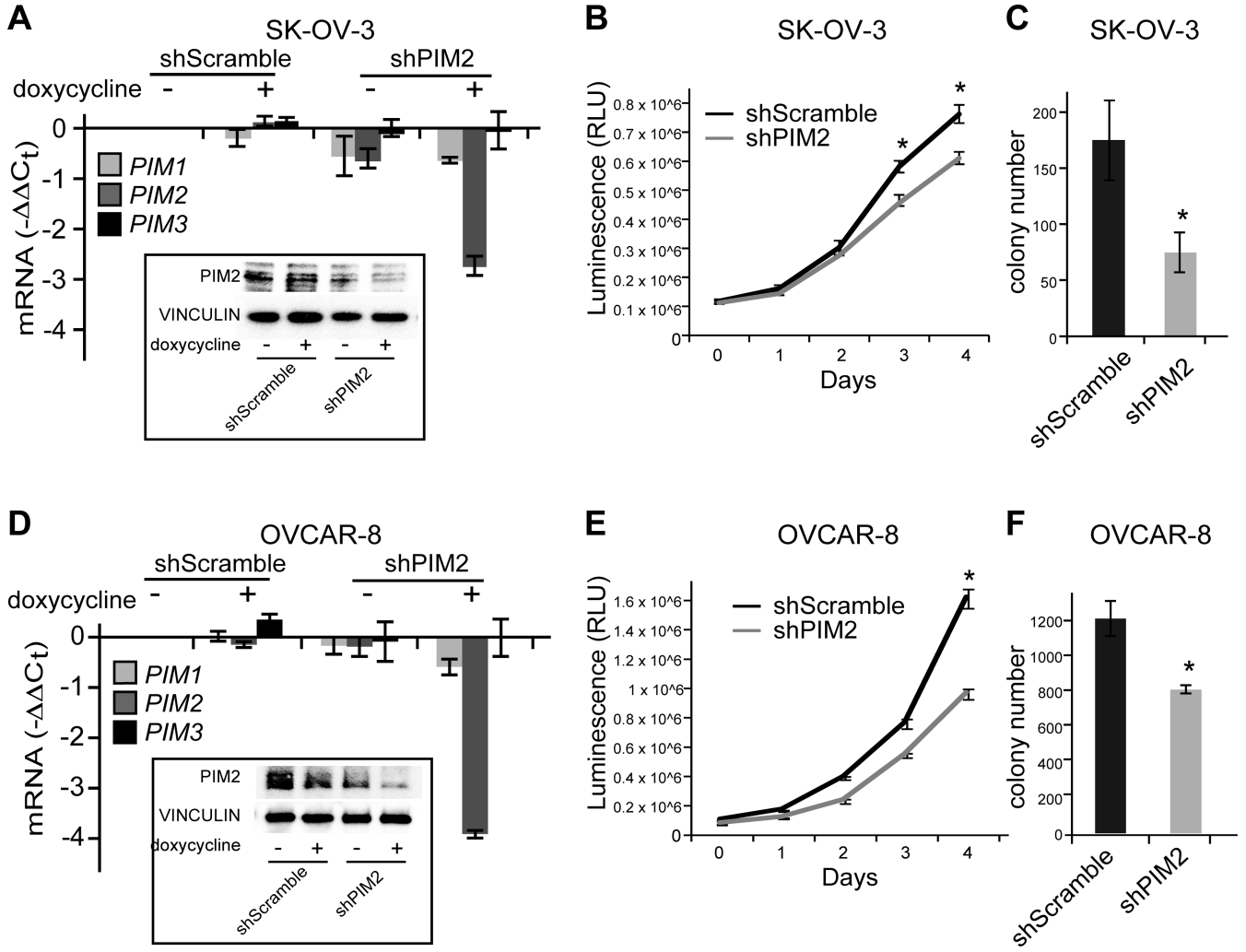

Figure 5. (A, D) PIM2 knockdown to study clonogenic ability of ovarian cancer cells. PIM2 silencing at both mRNA and protein levels in SK-OV-3 (A) and OVCAR-8 (D) cells triggered by doxycycline treatment (500 ng/mL) after stable transduction with lentiviral particles carrying PIM2-specific short hairpin (shPIM2) sequence under a Tet-on inducible promoter. Panels also show that mRNAs of *PIM1* and *PIM3* genes were not affected. As a control, cells were transduced with lentiviral particles carrying a nontargeting short hairpin sequence (shScramble). Growth curves of SK-OV-3 (B) and OVCAR-8 (E) cells after PIM2 silencing. Colony forming ability in soft-agar of SK-OV-3 (C) and OVCAR-8 (F) cells after PIM2 silencing. In this experiment, doxycycline was added every 4 days to both control (shScramble) and PIM2-silenced (shPIM2) cells for the duration of the experiment (2 weeks for OVCAR-8 cells and 4 weeks for SK-OV-3 cells). Colonies were stained with tetrazolium salts (MTT) and counted using ImageJ software. Statistical significance was determined using ANOVA test: $*P < 0.05$.

increased cell ability to form colonies in semisolid medium (Figure 7C), in agreement with its role as a pro-oncogenic kinase.

We queried The Cancer Genome Atlas to evaluate the status of the PIM2 gene in ovarian cancer samples.[35] Interestingly, the PIM2 gene was amplified in a significant fraction of the 580 naïve high-grade serous carcinomas of the ovary analyzed, which was more than in any other cancer histotype (see the Experimental Procedures for the relevant URLs).

Altogether, our data show that the PIM2 kinase is induced by DNA damaging agents in ovarian cancer cells and might interfere with apoptosis induced by platinum drugs likely via regulation of BAD phosphorylation.

DISCUSSION

We describe here a system-wide approach to decipher sensitivity/resistance of cancer cells to platinum. The CDDP-regulated proteome and phosphoproteome revealed an unexpected activation of the PIM2 kinase, not previously identified as a factor regulated by CDDP and involved in the cells response to the drug. This suggests that PIM2 kinase is a potential target to sensitize cells to platinum drugs.

As expected, the top 50 CDDP-induced phosphosites include a number of known direct targets of ATM and ATR, as also reported in a phosphoproteomic analysis of embryonic stem cells, i.e., cells with uncompromised DNA damage response, treated for a short time with CDDP.[5] Among them, we found H2A.X, which is involved in the initial enzymatic processing step of the DNA damage response. Its phosphorylation on Ser139 is a measure of double-strand breaks (DSBs)[36] and is required for signaling the recruitment of DNA repair proteins to DSBs. The other hyper-phosphorylated ATM substrate in our data, the transcriptional repressor TRIM28/KAP1, plays a key role in DNA repair when phosphorylated.[24] The upregulation of kinases involved in the MAPK (mitogen activated protein kinase) pathway, such as ERK1/2 and p90RSK, was also expected, as they are critical components of the signaling network activated by CDDP.[5,37] Moreover, our

dx.doi.org/10.1021/pr500651n | J. Proteome Res. 2014, 13, 4970−4982

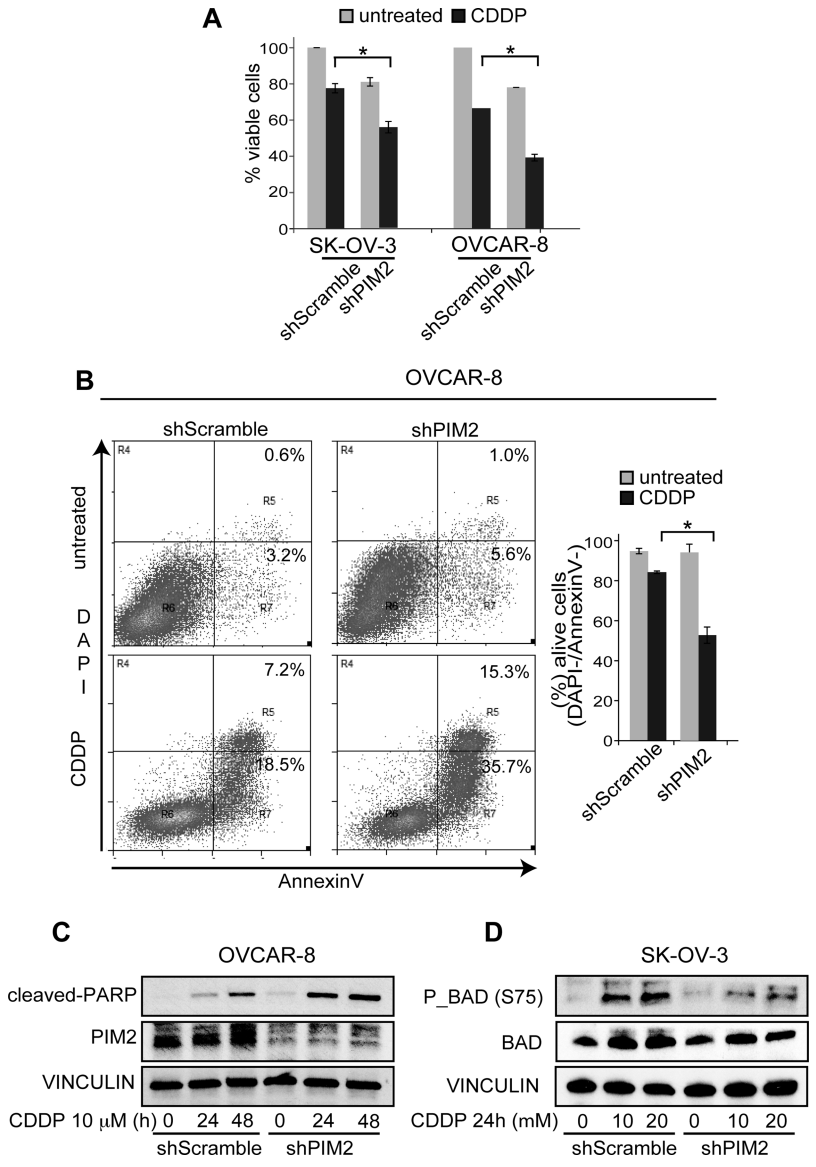

Figure 6. (A) Viability of control and PIM2-silenced cells in response to CDDP (4 μM for 48 h). Cell viability was measured with CellTiter Glo assay (mean ± standard deviation, $n = 3$). In the cell viability and apoptosis assays (see below), cells were grown in the presence of doxycycline. (B) Apoptosis assay: after CDDP treatment (10 μM for 72 h), both control and PIM2-silenced cells were labeled with Annexin V and DAPI and analyzed by flow cytometry (left panels). The percentage of early (R7) and late (R5) apoptotic cells is indicated in the windows of a representative experiment. The bar graph (right panel) shows the percentage of living (Annexin V and DAPI double negative) cells following the indicated treatments (mean ± standard deviation, $n = 3$). (C) Western blot analysis showing PARP cleavage upon CDDP treatment (10 μM for 24 and 48 h) in control and PIM2-silenced cells grown in the presence of doxycycline. (D) Western blot analysis showing BAD phosphorylation upon CDDP treatment (10 μM and 20 μM for 24 h) in control and PIM2-silenced cells grown in the presence of doxycycline. The blots were reprobed with vinculin antibody to confirm equal loading. Statistical significance was determined using ANOVA test: *$P < 0.05$.

data confirmed the activation of p38MAPK upon cell treatment with CDDP, in accordance with our previous work,[17] which is a necessary component of the pathway controlling cell cycle arrest and survival in p53-defective cells, such as the SK-OV-3 cells.[38] Similarly, an RNAi screen of the kinome identified ATR and its substrate CHK1 and members of the MAPK family as the kinases mostly involved in susceptibility to CDDP of SK-OV-3 cells.[39]

The bioinformatics analysis of phosphosites suggested that PIM2 kinase is a possible target of CDDP. Biochemical data showed that the PIM2 kinase was, indeed, induced by treating the cells with CDDP. This was reminiscent of the PIM2 induction associated with UV-induced DNA damage.[40] The PIM proteins are a family of short-lived serine/threonine kinases that are highly conserved throughout evolution in multicellular organisms.[29,30] In most species, this family consists of three different members (PIM1, PIM2, and PIM3) that show high homology and share substrate specificity. It is generally thought that PIM kinases do not require post-translational modifications to induce their kinase activity. They are constitutively active,[41] and their induction is largely regulated at the transcriptional and translational levels.[29,30]

PIM2 is an oncogenic kinase that is overexpressed in a range of hematopoietic malignancies and solid cancers.[29,30,42,43] It has already been shown that PIM kinases exert their oncogenic activities in many ways, such as by phosphorylating BAD and thus inhibiting its pro-apoptotic activity.[44] On the other hand, it has been reported that in human ovarian cancer cells

dx.doi.org/10.1021/pr500651n | J. Proteome Res. 2014, 13, 4970−4982

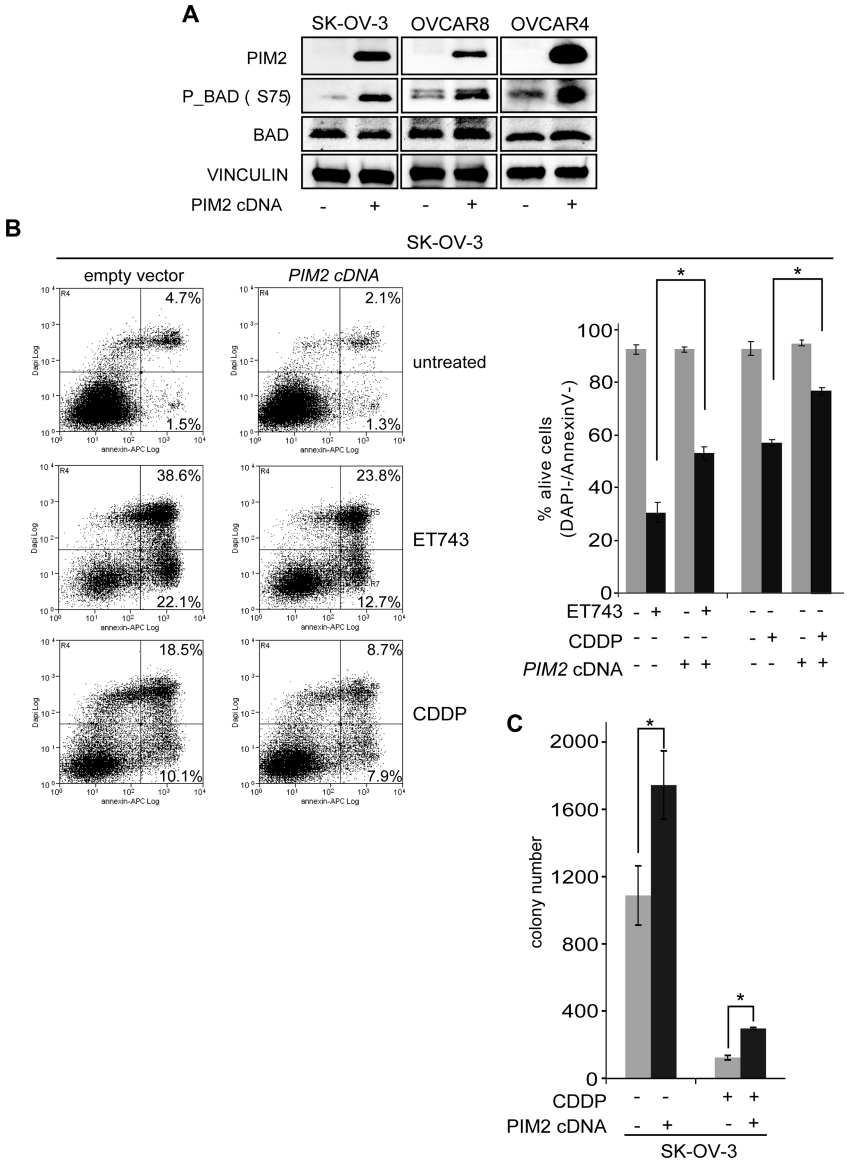

Figure 7. (A) Overexpression of PIM2 and BAD phosphorylation at Ser75 in ovarian cancer cells lines. The blots were reprobed with vinculin antibody to confirm equal loading. (B) Apoptosis assay: after either CDDP (10 μM for 72 h) or trabectedin (ET743 0.5 nM for 72 h) treatment, both empty vector and PIM2-overexpressing cells were labeled with Annexin V and DAPI and analyzed by flow cytometry (left panel). In these panels, the percentage of early (R7) and late (R5) apoptotic cells are indicated in the windows of a representative experiment. The bar graph (right panel) shows the percentage of living (Annexin V and DAPI double negative) cells following the indicated treatments (mean ± standard deviation, n = 3). (C) Graph showing the number of colonies formed by empty-vector and PIM2-overexpressing SK-OV-3 cells grown for 40 days in semisolid medium (soft-agar assay) both in the presence or in the absence of CDDP (5 μM). Colonies were stained with tetrazolium salts (MTT) and counted using ImageJ software. Statistical significance was determined using ANOVA test: *P < 0.05.

phosphorylation of BAD at serine 75 and serine 99 (known as Ser112 and Ser136, respectively, in mouse bad) is stimulated by CDDP and that these phosphorylation events rely on the MAPK/ERK and PI3K/AKT signaling pathways, respectively.[45] Our findings highlight the role of PIM2 kinase as a new player contributing to the CDDP-triggered phosphorylation of human BAD in ovarian cancer cells.

Clinically, BAD phosphorylation has been found to determine ovarian cancer chemosensitivity and patient survival.[46] Here, we show that PIM2 kinase overexpression partially protects ovarian cancer cells from DNA damaging agents, likely via the induction of BAD phosphorylation, and that targeting PIM2 by either biochemical inhibitors or RNA interference sensitizes cells to CDDP, impairing drug-triggered BAD phosphorylation. Moreover, the data shown here demonstrate that the PIM2 oncogenic kinase also triggers anchorage-independent proliferation of ovarian cancer cells. These findings are important because some PIM kinase inhibitors (AZD1208 and LGH447) are undergoing clinical trials for hematological and solid cancers and several others are under development.

We have studied the response of the SK-OV-3 ovarian cancer cells to CDDP and validated our data in a panel of ovarian cancer cell lines representative of different histotypes of ovarian cancer. At diagnosis, the majority of ovarian cancer patients present with an advanced disease and show a 5 year survival rate of 30%. Currently, cytoreductive surgery combined with chemotherapy based on platinum drugs and taxanes is the

dx.doi.org/10.1021/pr500651n | J. Proteome Res. 2014, 13, 4970−4982

standard treatment. Approximately 70% of patients respond to first-line chemotherapy, with the others being inherently platinum refractory. Moreover, approximately 70% of platinum-sensitive patients develop resistance later, suffer recurrence of disease, and eventually die. Therefore, the most critical issues in the therapy of advanced ovarian cancer are primary and acquired resistance to platinum-based treatments.

CONCLUSIONS

We provide the first quantitative and global phosphoproteomic analysis of an ovarian cancer cell line exposed to a platinum compound. This led to the identification of PIM2 as a candidate target kinase, predicted by contextual analysis of phosphosites. Functional validation showed that, in a number of ovarian cancer cell lines, PIM2 is involved in controlling cell growth and survival and response to DNA-damaging chemotherapeutics. Importantly, the PIM kinases are druggable and clinically viable inhibitors that are undergoing trials. Therefore, PIM kinase target therapy is a potential avenue to improve platinum sensitivity and to reverse resistance to platinum.

ASSOCIATED CONTENT

Supporting Information

Clustering analysis of the pS, pT, and pY containing peptides; biochemical and functional validation of kinases activated/inhibited by CDDP treament; pS, pT, and pY peptides purified using FASP/SCX/TiO_2 from SK-OV-3 cells treated ± HGF and ± CDDP; and unique proteins identified in the in-gel digestion samples from SK-OV-3 cells treated ± HGF and ± CDDP. This material is available free of charge via the Internet at http://pubs.acs.org.

AUTHOR INFORMATION

Corresponding Author

*Phone: +390119933343. Fax: +390119933417. E-mail: mariaflavia.direnzo@unito.it.

Present Addresses

[‖]Protein Function Group, University of Liverpool, Institute of Integrative Biology, L69 7ZB Liverpool, United Kingdom.
[⊥]Department of Experimental Oncology, European Institute of Oncology, Via Adamello 16, 20136 Milano, Italy.

Notes

The authors declare no competing financial interest.

ACKNOWLEDGMENTS

This work has been supported by grants to M.F.D.: AIRC 2012 IG grant n°13050, grant of the CARIPLO Foundation, and grant of the Progetto di Ateneo−Compagnia di San Paolo n° ORTO11RKTW.

REFERENCES

(1) Lebwohl, D.; Canetta, R. Clinical development of platinum complexes in cancer therapy: an historical perspective and an update. *Eur. J. Cancer* **1998**, *34*, 1522−34.

(2) Jamieson, E. R.; Lippard, S. J. Structure, recognition, and processing of cisplatin−DNA adducts. *Chem. Rev.* **1999**, *99*, 2467−98.

(3) Galluzzi, L.; Senovilla, L.; Vitale, I.; Michels, J.; Martins, I.; Kepp, O.; Castedo, M.; Kroemer, G. Molecular mechanisms of cisplatin resistance. *Oncogene* **2012**, *31*, 1869−83.

(4) Bartek, J.; Lukas, J. DNA damage checkpoints: from initiation to recovery or adaptation. *Curr. Opin. Cell Biol.* **2007**, *19*, 238−45.

(5) Pines, A.; Kelstrup, C. D.; Vrouwe, M. G.; Puigvert, J. C.; Typas, D.; Misovic, B.; de Groot, A.; von Stechow, L.; van de Water, B.; Danen, E. H.; Vrieling, H.; Mullenders, L. H.; Olsen, J. V. Global phosphoproteome profiling reveals unanticipated networks responsive to cisplatin treatment of embryonic stem cells. *Mol. Cell. Biol.* **2011**, *31*, 4964−77.

(6) Reinhardt, H. C.; Yaffe, M. B. Kinases that control the cell cycle in response to DNA damage: Chk1, Chk2, and MK2. *Curr. Opin. Cell Biol.* **2009**, *21*, 245−55.

(7) Omerovic, J.; Hammond, D. E.; Prior, I. A.; Clague, M. J. Global snapshot of the influence of endocytosis upon EGF receptor signaling output. *J. Proteome Res.* **2012**, *11*, 5157−66.

(8) Wiśniewski, J. R.; Zougman, A.; Nagaraj, N.; Mann, M. Universal sample preparation method for proteome analysis. *Nat. Methods* **2009**, *6*, 359−62.

(9) Olsen, J. V.; Blagoev, B.; Gnad, F.; Macek, B.; Kumar, C.; Mortensen, P.; Mann, M. Global, in vivo, and site-specific phosphorylation dynamics in signaling networks. *Cell* **2006**, *127*, 635−48.

(10) Cox, J.; Neuhauser, N.; Michalski, A.; Scheltema, R. A.; Olsen, J. V.; Mann, M. Andromeda: a peptide search engine integrated into the MaxQuant environment. *J. Proteome Res.* **2011**, *10*, 1794−805.

(11) Cox, J.; Mann, M. MaxQuant enables high peptide identification rates, individualized p.p.b.-range mass accuracies and proteome-wide protein quantification. *Nat. Biotechnol.* **2008**, *26*, 1367−72.

(12) Rigbolt, K. T.; Vanselow, J. T.; Blagoev, B. GProX, a user-friendly platform for bioinformatics analysis and visualization of quantitative proteomics data. *Mol. Cell. Proteomics* **2011**, *10*, O110.007450.

(13) Futschik, M. E.; Carlisle, B. Noise-robust soft clustering of gene expression time-course data. *J. Bioinf. Comput. Biol.* **2005**, *3*, 965−88.

(14) Rigbolt, K. T.; Prokhorova, T. A.; Akimov, V.; Henningsen, J.; Johansen, P. T.; Kratchmarova, I.; Kassem, M.; Mann, M.; Olsen, J. V.; Blagoev, B. System-wide temporal characterization of the proteome and phosphoproteome of human embryonic stem cell differentiation. *Sci. Signaling* **2011**, *4*, rs3.

(15) Schwartz, D.; Gygi, S. P. An iterative statistical approach to the identification of protein phosphorylation motifs from large-scale data sets. *Nat. Biotechnol.* **2005**, *23*, 1391−8.

(16) Linding, R.; Jensen, L. J.; Pasculescu, A.; Olhovsky, M.; Colwill, K.; Bork, P.; Yaffe, M. B.; Pawson, T. NetworKIN: a resource for exploring cellular phosphorylation networks. *Nucleic Acids Res.* **2008**, *36*, D695−9.

(17) Coltella, N.; Rasola, A.; Nano, E.; Bardella, C.; Fassetta, M.; Filigheddu, N.; Graziani, A.; Comoglio, P. M.; Di Renzo, M. F. p38 MAPK turns hepatocyte growth factor to a death signal that commits ovarian cancer cells to chemotherapy-induced apoptosis. *Int. J. Cancer.* **2006**, *118*, 2981−90.

(18) Bardella, C.; Dettori, D.; Olivero, M.; Coltella, N.; Mazzone, M.; Di Renzo, M. F. The therapeutic potential of hepatocyte growth factor to sensitize ovarian cancer cells to cisplatin and paclitaxel in vivo. *Clin. Cancer Res.* **2007**, *13*, 2191−8.

(19) Cerami, E.; Gao, J.; Dogrusoz, U.; Gross, B. E.; Sumer, S. O.; Aksoy, B. A.; Jacobsen, A.; Byrne, C. J.; Heuer, M. L.; Larsson, E.; Antipin, Y.; Reva, B.; Goldberg, A. P.; Sander, C.; Schultz, N. The cBio cancer genomics portal: an open platform for exploring multidimensional cancer genomics data. *Cancer Discovery* **2012**, *2*, 401−4.

(20) Choudhary, C.; Mann, M. Decoding signalling networks by mass spectrometry-based proteomics. *Nat. Rev. Mol. Cell Biol.* **2010**, *11*, 427−39.

(21) Xiang, Y.; Ma, N.; Wang, D.; Zhang, Y.; Zhou, J.; Wu, G.; Zhao, R.; Huang, H.; Wang, X.; Qiao, Y.; Li, F.; Han, D.; Wang, L.; Zhang, G.; Gao, X. MiR-152 and miR-185 co-contribute to ovarian cancer cells cisplatin sensitivity by targeting DNMT1 directly: a novel epigenetic therapy independent of decitabine. *Oncogene* **2013**, *33*, 378−86.

(22) Zhang, X.; Samadi, A. K.; Roby, K. F.; Timmermann, B.; Cohen, M. S. Inhibition of cell growth and induction of apoptosis in ovarian

carcinoma cell lines CaOV3 and SKOV3 by natural withanolide Withaferin A. *Gynecol. Oncol.* **2012**, *124*, 606−12.
(23) Rasola, A.; Anguissola, S.; Ferrero, N.; Gramaglia, D.; Maffe, A.; Maggiora, P.; Comoglio, P. M.; Di Renzo, M. F. Hepatocyte growth factor sensitizes human ovarian carcinoma cell lines to paclitaxel and cisplatin. *Cancer Res.* **2004**, *64*, 1744−50.
(24) Hu, C.; Zhang, S.; Gao, X.; Xu, X.; Lv, Y.; Zhang, Y.; Zhu, Z.; Zhang, C.; Li, Q.; Wong, J.; Cui, Y.; Zhang, W.; Ma, L.; Wang, C. Roles of kruppel-associated box (KRAB)-associated co-repressor KAP1 Ser-473 phosphorylation in DNA damage response. *J. Biol. Chem.* **2012**, *287*, 18937−52.
(25) Johnson, L. N.; Noble, M. E.; Owen, D. J. Active and inactive protein kinases: structural basis for regulation. *Cell* **1996**, *85*, 149−58.
(26) Pegram, M. D.; Lipton, A.; Hayes, D. F.; Weber, B. L.; Baselga, J. M.; Tripathy, D.; Baly, D.; Baughman, S. A.; Twaddell, T.; Glaspy, J. A.; Slamon, D. J. Phase II study of receptor-enhanced chemosensitivity using recombinant humanized anti-p185HER2/neu monoclonal antibody plus cisplatin in patients with HER2/neu-overexpressing metastatic breast cancer refractory to chemotherapy treatment. *J. Clin. Oncol.* **1998**, *16*, 2659−71.
(27) Price, P. M.; Yu, F.; Kaldis, P.; Aleem, E.; Nowak, G.; Safirstein, R. L.; Megyesi, J. Dependence of cisplatin-induced cell death in vitro and in vivo on cyclin-dependent kinase 2. *J. Am. Soc. Nephrol.* **2006**, *17*, 2434−42.
(28) Xia, Y.; Yang, W.; Bu, W.; Ji, H.; Zhao, X.; Zheng, Y.; Lin, X.; Li, Y.; Lu, Z. Differential regulation of c-Jun protein plays an instrumental role in chemoresistance of cancer cells. *J. Biol. Chem.* **2013**, *288*, 19321−9.
(29) Blanco-Aparicio, C.; Carnero, A. Pim kinases in cancer: diagnostic, prognostic and treatment opportunities. *Biochem. Pharmacol.* **2013**, *85*, 629−43.
(30) Nawijn, M. C.; Alendar, A.; Berns, A. For better or for worse: the role of Pim oncogenes in tumorigenesis. *Nat. Rev. Cancer* **2011**, *11*, 23−34.
(31) Chen, L. S.; Redkar, S.; Bearss, D.; Wierda, W. G.; Gandhi, V. Pim kinase inhibitor, SGI-1776, induces apoptosis in chronic lymphocytic leukemia cells. *Blood* **2009**, *114*, 4150−7.
(32) Chang, M.; Kanwar, N.; Feng, E.; Siu, A.; Liu, X.; Ma, D.; Jongstra, J. PIM kinase inhibitors downregulate STAT3(Tyr705) phosphorylation. *Mol. Cancer Ther.* **2010**, *9*, 2478−87.
(33) Zhang, Y.; Wang, Z.; Li, X.; Magnuson, N. S. Pim kinase-dependent inhibition of c-Myc degradation. *Oncogene* **2008**, *27*, 4809−19.
(34) Zippo, A.; De Robertis, A.; Serafini, R.; Oliviero, S. PIM1-dependent phosphorylation of histone H3 at serine 10 is required for MYC-dependent transcriptional activation and oncogenic transformation. *Nat. Cell Biol.* **2007**, *9*, 932−44.
(35) Network, C. G. A. R. Integrated genomic analyses of ovarian carcinoma. *Nature* **2011**, *474*, 609−15.
(36) Takahashi, A.; Ohnishi, T. Does gammaH2AX foci formation depend on the presence of DNA double strand breaks? *Cancer Lett.* **2005**, *229*, 171−9.
(37) Brozovic, A.; Osmak, M. Activation of mitogen-activated protein kinases by cisplatin and their role in cisplatin-resistance. *Cancer Lett.* **2007**, *251*, 1−16.
(38) Reinhardt, H. C.; Aslanian, A. S.; Lees, J. A.; Yaffe, M. B. p53-deficient cells rely on ATM- and ATR-mediated checkpoint signaling through the p38MAPK/MK2 pathway for survival after DNA damage. *Cancer Cell* **2007**, *11*, 175−89.
(39) Arora, S.; Bisanz, K. M.; Peralta, L. A.; Basu, G. D.; Choudhary, A.; Tibes, R.; Azorsa, D. O. RNAi screening of the kinome identifies modulators of cisplatin response in ovarian cancer cells. *Gynecol. Oncol.* **2010**, *118*, 220−7.
(40) Zirkin, S.; Davidovich, A.; Don, J. The PIM-2 kinase is an essential component of the ultraviolet damage response that acts upstream to E2F-1 and ATM. *J. Biol. Chem.* **2013**, *288*, 21770−83.
(41) Qian, K. C.; Wang, L.; Hickey, E. R.; Studts, J.; Barringer, K.; Peng, C.; Kronkaitis, A.; Li, J.; White, A.; Mische, S.; Farmer, B. Structural basis of constitutive activity and a unique nucleotide binding mode of human Pim-1 kinase. *J. Biol. Chem.* **2005**, *280*, 6130−7.
(42) Brault, L.; Gasser, C.; Bracher, F.; Huber, K.; Knapp, S.; Schwaller, J. PIM serine/threonine kinases in the pathogenesis and therapy of hematologic malignancies and solid cancers. *Haematologica* **2010**, *95*, 1004−15.
(43) Kapelko-Słowik, K.; Urbaniak-Kujda, D.; Wołowiec, D.; Jaźwiec, B.; Dybko, J.; Jakubaszko, J.; Słowik, M.; Kuliczkowski, K. Expression of PIM-2 and NF-κB genes is increased in patients with acute myeloid leukemia (AML) and acute lymphoblastic leukemia (ALL) and is associated with complete remission rate and overall survival. *Postepy Hig Med. Dosw.* **2013**, *67*, 553−9.
(44) Fox, C. J.; Hammerman, P. S.; Cinalli, R. M.; Master, S. R.; Chodosh, L. A.; Thompson, C. B. The serine/threonine kinase Pim-2 is a transcriptionally regulated apoptotic inhibitor. *Genes Dev.* **2003**, *17*, 1841−54.
(45) Hayakawa, J.; Ohmichi, M.; Kurachi, H.; Kanda, Y.; Hisamoto, K.; Nishio, Y.; Adachi, K.; Tasaka, K.; Kanzaki, T.; Murata, Y. Inhibition of BAD phosphorylation either at serine 112 via extracellular signal-regulated protein kinase cascade or at serine 136 via Akt cascade sensitizes human ovarian cancer cells to cisplatin. *Cancer Res.* **2000**, *60*, 5988−94.
(46) Marchion, D. C.; Cottrill, H. M.; Xiong, Y.; Chen, N.; Bicaku, E.; Fulp, W. J.; Bansal, N.; Chon, H. S.; Stickles, X. B.; Kamath, S. G.; Hakam, A.; Li, L.; Su, D.; Moreno, C.; Judson, P. L.; Berchuck, A.; Wenham, R. M.; Apte, S. M.; Gonzalez-Bosquet, J.; Bloom, G. C.; Eschrich, S. A.; Sebti, S.; Chen, D. T.; Lancaster, J. M. BAD phosphorylation determines ovarian cancer chemosensitivity and patient survival. *Clin. Cancer Res.* **2011**, *17*, 6356−66.